

1 Terahertz multi-film material parameter extraction 2 using gradient descent algorithms

3 THEO SMITH¹, ARTA LATIFI² NICHOLAS T. KLOKKOU,¹ BEN
4 BEDDOES,^{1,*}, JON GORECKI², GEORGIOS BARMPPARIS, VASILIS
5 APOSTOLOPOULOS^{5,6,1}

6 ¹*School of Physics and Astronomy, University of Southampton, United Kingdom*

7 ²*Royal School of Mines, Imperial College London, United Kingdom*

8 *Germany*

9 ⁵*University of Crete, Department of Physics, Heraklion, GR-70013, Greece*

10 ⁶*Foundation for Research and Technology-Hellas, Institute of electronic structure and Laser, Heraklion,*
11 *Crete*

12 ⁴*Optoelectronics Research Centre, University of Southampton, United Kingdom*

13 ^{*}scr1n19@soton.ac.uk

14 **Abstract:** Terahertz time domain spectroscopy is a technique to examine the properties of
15 materials using THz radiation. Extracting these properties from experimental data can be unstable
16 and laborious, especially when the data contains multiple reflections, such as in thin or multi-layer
17 samples. In these cases, traditional extraction algorithms typically fail as there are too many free
18 parameters to solve for. Here we develop an extraction method that allows for stable and accurate
19 extraction of material parameters from multi-layer samples. Our method utilises a combination
20 of Bayesian optimization and gradient descent algorithms operating in the time domain. We
21 test these optimization algorithms on both simulated and experimental data, demonstrating their
22 ability to extract sample parameters from multi-layer systems without prior knowledge of the
23 samples. **Our method will be good for some practical reasons and examples of things that it**
24 **would be good for and why people want to us it.**

25 1. Introduction

26 Terahertz Time Domain Spectroscopy (THz-TDS) is a powerful analytical technique for deter-
 27 mining the complex optical properties of materials. Importantly, THz-TDS has an advantage over
 28 nearly all spectroscopic methods in that it is able to directly measure the time varying electric
 29 field of the electromagnetic pulse, as opposed to simply sampling the time averaged magnitude,
 30 thereby retaining information on the phase of the electric field components. Due to this fact,
 31 THz-TDS is able to determine the complex frequency-dependent optical parameters of a material
 32 (either refractive index, conductivity, or permittivity) without having to rely on approximations or
 33 assumptions. The analysis of material spectra generally involves fitting the experimental data to
 34 a theoretical transfer function, and modifying the material properties to minimise the difference
 35 between theory and experiment. For the simplest case of a flat, homogeneous, single-layer,
 36 optically thick (thickness $> \lambda_0$) sample the existing THz-TDS fitting routines are extremely
 37 stable and generally converge on a single solution within a few iterations. However, many
 38 samples do not satisfy this list of prerequisites, and once the sample geometry becomes more
 39 complicated (such as for thin or multi-layer samples) the transfer functions produce multiple
 40 mathematically-valid solutions; numerical fitting routines encounter non-convex loss functions,
 41 multiple local minima appear, and therefore determining the true material parameters becomes
 42 challenging.

43 what is the angle for this introduction? are we saying that we are borrowing the optimisation
 44 algorithms from ML, and then using them in a more traditional setting?

46 Material parameter extraction can be formulated as an inverse problem. Simplifying the
 47 problem of a multi-layered sample by assuming a discrete, frequency independent, complex
 48 refractive index for each layer. This reduces the number of free parameters being solved for.
 49 In this framework, a forward model maps a set of material parameters to a predicted system
 50 response in our case, producing the time-domain sample pulse given the material parameters
 51 and a measured reference pulse. The inverse problem is then solved by adjusting the material
 52 parameters until the model output matches the experimental data within a defined tolerance. This
 53 approach implicitly assumes that the forward model provides an accurate physical description of
 54 the system, making the choice of model particularly one suited to the sample geometry critical
 55 to obtaining meaningful results. The existing methods typically use the Fresnel model of light
 56 propagating through a sample to construct a theoretical transfer function from n and k .

$$H_{\text{theoretical}} = \frac{4\tilde{n}}{(\tilde{n} + 1)^2} e^{-\frac{i(\tilde{n}-1)\omega d}{c}}, \quad (1)$$

57 An objective function is then constructed using this and the experimental data.

$$f(\tilde{n}, \omega) = \ln(H_{\text{theoretical}}) - \ln(H_{\text{experimental}}) \quad (2)$$

58 The root of this objective function ($f(\tilde{n}, \omega)$) with respect to \tilde{n} is the solution to this inverse
 59 problem. The root is found using Newton's method, an iterative root finding algorithm that uses
 60 the following parameter update rule.

$$\tilde{n}_{t+1} = \tilde{n}_t - \frac{f(\tilde{n}_t)}{f'(\tilde{n}_t)} \quad (3)$$

61 This works well for basic geometries but modified versions for thin samples with reflections or
 62 multiple layers struggle to stably converge to a single solution. In this work, we are not using
 63 the Fresnel model, opting instead for a forward model based on the matrix transfer method [1].
 64 This allows the model to produce data for samples with multiple layers. Given the complexity of
 65 solving the objective function with this method, we dispense with Newton's method in favour of

66 gradient descent. This means we do not require an analytical derivative of the objective with
 67 respect to the forward models parameters. This is commonly used in deep learning to train neural
 68 networks to fit their training data. The basic gradient descent algorithm uses the parameter update
 69 rule below for a sample with N layers.

$$\theta_{t+1} = \theta_t - \eta \nabla_{\theta} \mathcal{L}(\theta_t) \quad (4)$$

70
 71 where $\theta = \{\theta_1, \theta_2, \dots, \theta_N\}$ with each $\theta_j = \{n_j, k_j, d_j\}$ for $j = 1, \dots, N$.

72 θ is the parameter set being updated and $\mathcal{L}(\theta_t)$ describes the objective function, t indicates the
 73 optimization step and η is a learning rate (an arbitrary constant).

74 For gradient descent to be used, the forward model must also be differentiable with respect to
 75 it's input parameters. This means functions such as phase unwrapping cannot be used because
 76 this is a discontinuous process. The objective here is to minimize the root mean squared error
 77 (rMSE) between the predicted time domain pulse and the experimental one. By doing this, we
 78 are fitting an average refractive index (w.r.t frequency) for each layer by calculating loss in the
 79 time domain.

80 1.1. Transfer Matrix methods for multilayer samples in THz-TDS

81 Any model composed of differentiable operations (e.g., as implemented in PyTorch) can, in
 82 principle, be optimized using gradient-based methods such as Adam. However, differentiability
 83 alone does not guarantee successful or accurate convergence due to potential issues such as
 84 non-convex loss landscapes, ill-conditioned gradients, or sensitivity to initial parameter values.
 85 In this work, the transfer matrix method (TMM) is adopted as the forward model, owing to its
 86 ability to compute the total transmission and reflection from stratified media with high physical
 87 fidelity. TMM provides a well-established, physically grounded framework that integrates
 88 well into a differentiable pipeline, enabling parameter inference for multi-layered structures via
 89 backpropagation.

91 This approach is based on the transfer matrix method (TMM) [1], a well-established technique
 92 for modeling wave propagation in stratified media. At each interface between layers, a portion of
 93 the incident THz pulse is reflected and transmitted, while a phase shift is accumulated during
 94 propagation through each layer [2]. By enforcing electromagnetic boundary conditions namely,
 95 the continuity of the components of the electric and magnetic fields the reflection and transmission
 96 coefficients can be derived analytically for each interface. Consider a pulse propagating from an
 97 incident medium with refractive index n_0 into a layer with complex refractive index $n_j = n'_j + ik_j$
 98 and physical thickness d_j . The corresponding complex optical path length is given by $D_j = n_j \cdot d_j$.
 99 The single-layer reflection and transmission coefficients can then be expressed as [1]:

$$r = \frac{i}{2} \cdot \frac{\frac{n_0}{n_j} - \frac{n_j}{n_0}}{\cos(n_j D_j) + \frac{i}{2} \left(\frac{n_0}{n_j} + \frac{n_j}{n_0} \right) \sin(n_j D_j)} \quad (5)$$

$$t = \frac{1}{\cos(n_j D_j) + \frac{i}{2} \left(\frac{n_0}{n_j} + \frac{n_j}{n_0} \right) \sin(n_j D_j)} \quad (6)$$

100 These coefficients are computed for each layer in the sample. The overall reflection (R) and
 101 transmission (T) coefficients for the entire stack are then obtained by recursively combining the
 102 individual layer matrices using the standard TMM formulation. The complex transmission coeffi-
 103 cient T captures both amplitude attenuation and phase delay, thereby accounting for absorption
 104 and dispersion effects across the structure. This enables the simulation of time domain THz
 105 responses by applying the computed T to a reference pulse in the frequency domain, followed by
 106 an inverse Fourier transform.

107
 108 Once T is calculated, the sample's response to a reference pulse can be found. This is calculated
 109 in the frequency domain with an FFT (fast Fourier transform) to find $X(\omega)$. The frequency
 110 domain response is calculated using the transmission coefficient as the transfer function.

$$Y(\omega) = T(\omega) \cdot X(\omega) \quad (7)$$

111 An IFFT (inverse fast Fourier transform) is used to convert this back to the time domain $y(t)$.

$$y(t) = \mathcal{F}^{-1}[T(\omega) \cdot \mathcal{F}[x(t)]] \quad (8)$$

112 Figure 1 shows a completely simulated system with 3 layers $n = 2, 3, 2$ and $d = 1, 0.1, 1$ mm.

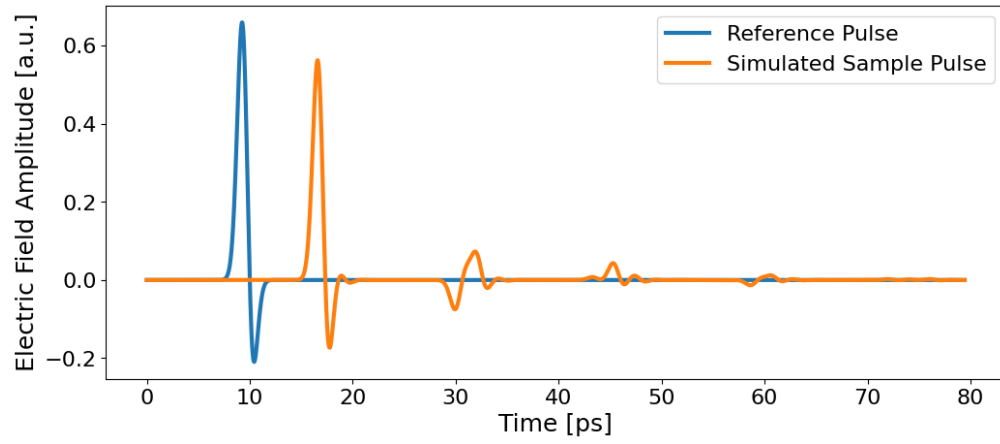


Fig. 1. Time domain of simulated reference and sample pulse for a 3 layered material with material parameters: $n = 2, 3, 2$ and $d = 1, 0.1, 1$ mm respectively. These were simulated using TMM.

113 1.2. Gradient descent for material parameter extraction

114 In order to fit for thickness at the same time as refractive index, we assume a constant refractive
 115 index across the frequency range. This will be addressed in future work. We have a discrete
 116 parameter set θ_j for each layer (j).

$$\theta_j = \{n_j, k_j, d_j\} \quad (9)$$

117 These parameters are passed to the TMM model to compute T giving $T(\theta)$. A prediction of
 118 the sample pulse from these parameters is obtained from equation 8.

$$\hat{y}(\theta) = \mathcal{F}^{-1}[T(\theta) \cdot \mathcal{F}[x(t)]] \quad (10)$$

119 We then construct a loss function to be minimized by a gradient based algorithm. Root mean
 120 squared error provides a lightweight and robust error metric for accurate comparison of the
 121 pulses.

$$L(\theta) = \sqrt{\frac{1}{N} \sum_{i=1}^N (y_{\text{sim}}(t_i; \theta) - y_{\text{exp}}(t_i))^2} \quad (11)$$

122 where N is the number of data points in the time domain, $y_{\text{exp}}(t_i)$ is the experimentally
 123 measured pulse and $y_{\text{sim}}(t_i; \theta)$ is the pulse simulated with TMM using parameters θ . Gradient
 124 descent updates parameters based on a learning rate and the gradient of the loss function with
 125 respect to the free parameters.

$$\theta_{t+1} = \theta_t - \eta \nabla_{\theta} \mathcal{L}(\theta_t) \quad (12)$$

126 η is the learning rate and helps to determine the rate and resolution of the fitting and t denotes
 127 the index of the iteration. The number of iterations and the learning rate depend on the loss
 128 landscape of the problem. This can be affected by the level of noise, number of parameters and
 129 the physical properties of the sample. To improve convergence stability and reduce sensitivity to
 130 manual hyperparameter tuning, we employ the Adam optimizer [3], a gradient-based method that
 131 adaptively adjusts the learning rate for each parameter. Adam tracks two exponential moving
 132 averages, the first and second moments (mean of gradients). These are computed and modified in
 133 the following way:

134 The first moment at step t :

$$m_t = \beta_1 m_{t-1} + (1 - \beta_1) \nabla_{\theta} \mathcal{L}(\theta_t) \quad (13)$$

135 and the second moment at step t :

$$v_t = \beta_2 v_{t-1} + (1 - \beta_2) (\nabla_{\theta} \mathcal{L}(\theta_t))^2 \quad (14)$$

136 These are bias corrected using:

$$\hat{m}_t = \frac{m_t}{1 - \beta_1}, \quad \hat{v}_t = \frac{v_t}{1 - \beta_2} \quad (15)$$

137 This leads to the overall parameter update rule:

$$\theta_{t+1} = \theta_t - \eta \frac{\hat{m}_t}{\sqrt{\hat{v}_t} + \epsilon} \quad (16)$$

138 Adam combines the advantages of momentum and RMSProp [3], making it well-suited for
 139 problems with noisy gradients or poorly scaled loss landscapes, such as those arising in inverse
 140 reconstruction of layered media.

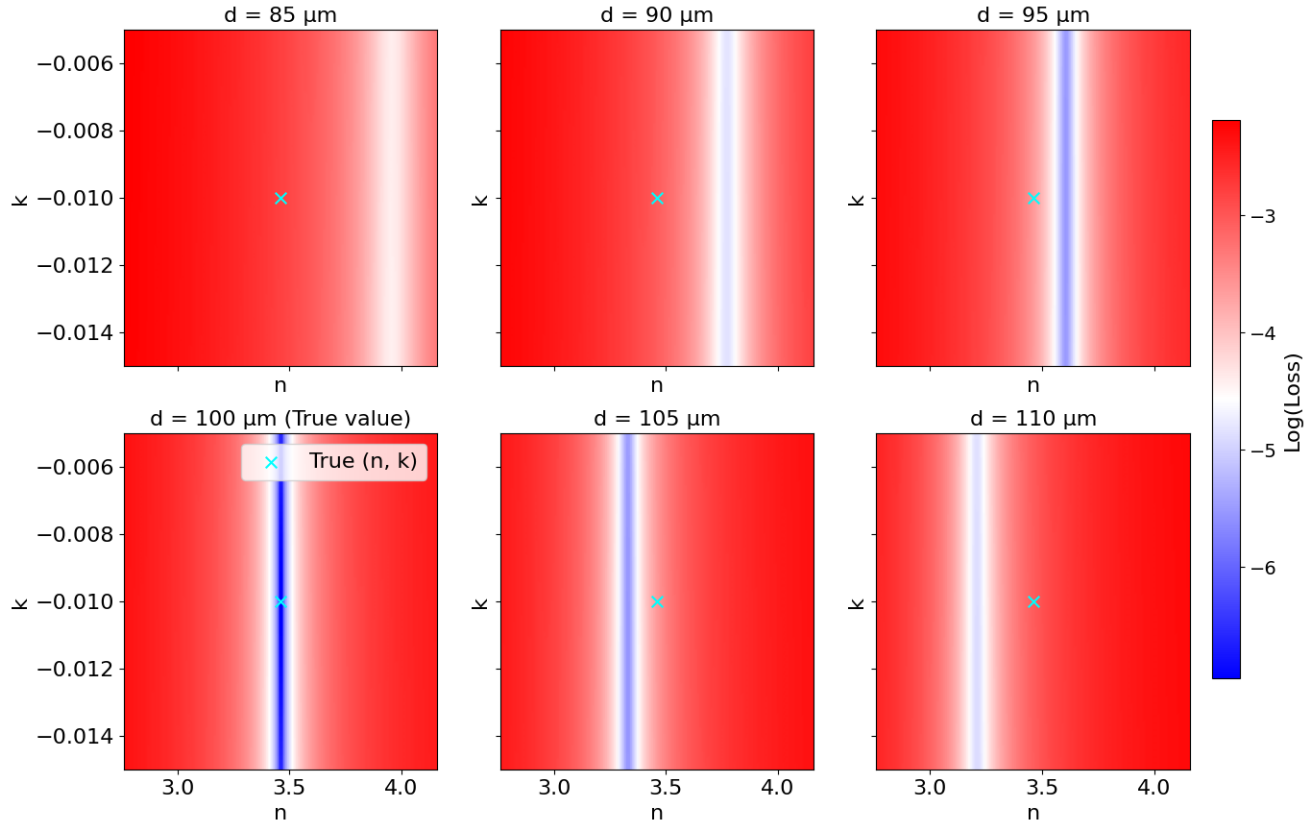


Fig. 2. Logarithmic loss landscapes as a function of refractive index parameters n and k for different assumed thickness values d . Each subplot corresponds to a fixed thickness between 85–110 μm . The black dot marks the true (n, k) . At the correct thickness ($d = 100 \mu\text{m}$, bottom left), the true values coincide with the minimum-loss region (blue). For mismatched thicknesses, the minimum-loss region shifts n , illustrating the coupling between thickness and refractive index in the fitting process. These regions also have a higher value of minimum loss, representing a poorer overall fitting than that with the correct thickness.

For the adam algorithm, the rate of convergence depends on the gradient of loss at that point in the parameter space. Initial guesses that are far from the correct values tend to have a flat gradient, as can be seen in Figure 2. Areas with low or no gradient cause the algorithm to need more steps to converge and in some cases, can prevent convergence all together. We are using Bayesian optimisation in order to speed up the gradient descent method and improve initial guess passed to the adam algorithm. Bayesian optimization is a global optimization strategy for expensive black-box functions. It models the objective using a probabilistic surrogate, typically a Gaussian Process [4]. Based on this model, it selects the next evaluation point by maximizing an acquisition function like Expected Improvement (EI) or Upper Confidence Bound [5, 6]. This method is particularly efficient in scenarios where function evaluations are costly. It has a range of uses including hyperparameter tuning for machine learning models [7]. The balance between exploration and exploitation is controlled explicitly through the acquisition function. Bayesian optimization provides an efficient method for searching wide parameter spaces with

155 a few features as in Figure 2. These parameters are then fine tuned using the gradient based
 156 method. Figure 3 shows the loss landscape at the correct thickness and zoomed into a smaller
 157 range of n values. This shows a clear gradient to a minimum value of loss that coincides with the
 158 true values of n and k . This landscape is optimal to be solved by gradient descent.

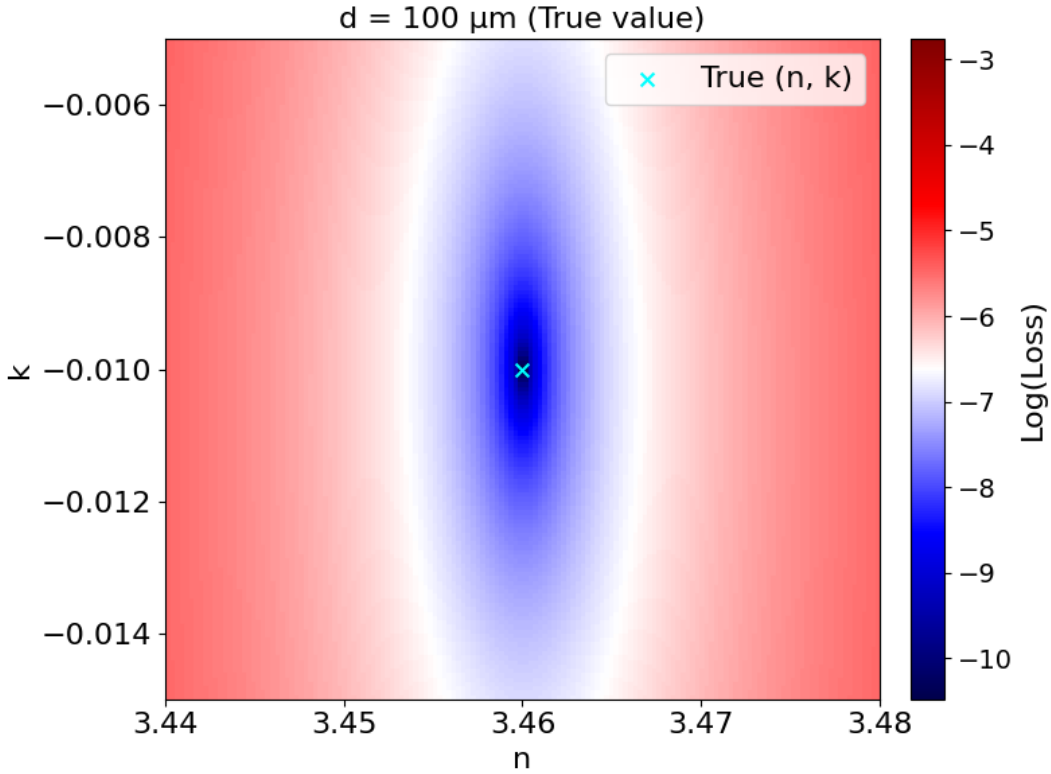


Fig. 3. Log-loss landscape for $d = 100 \mu\text{m}$ (true value). The refractive index axis is shown in a narrowed range, highlighting the steep gradient of the loss surface with respect to n and a visible gradient with respect to k .

159 In Figure 4 the time domain of simulated reference and sample pulse for a 2 layered material
 160 with material parameters: $n = 3.46 - 0.01j$, $2.5 - 0.015i$ and $d = 1, 0.2 \text{ mm}$ respectively is shown in
 161 4(a). These were simulated using a matrix transfer methods. In 4(b) the Bayesian optimisation
 162 results are shown where for the two layers we obtained $n = 3.466 - 0.005j$, $2.493 - 0.023j$. In Figure
 163 4(c) using the Bayesian as a first approximation the gradient descent converges to $3.4600 - 0.010j$,
 164 $2.50007 - 0.01501j$ which is close to the initial values. The Bayesian fitting stage allows for a
 165 fast and rough search of a wide parameter space for samples with largely unknown material
 166 parameters. In this case the search space ranged from n_1 : 2.67-3.67, k_1 : -0.025-0.005, d_1 :
 167 600-1200 μm for layer 1 and n_2 : 1.7-2.7, k_2 : -0.027-0.007, d_2 : 100-700 μm for layer 2. The
 168 values from this stage are then fine-tuned using the adam based algorithm to achieve a higher
 169 level of accuracy.

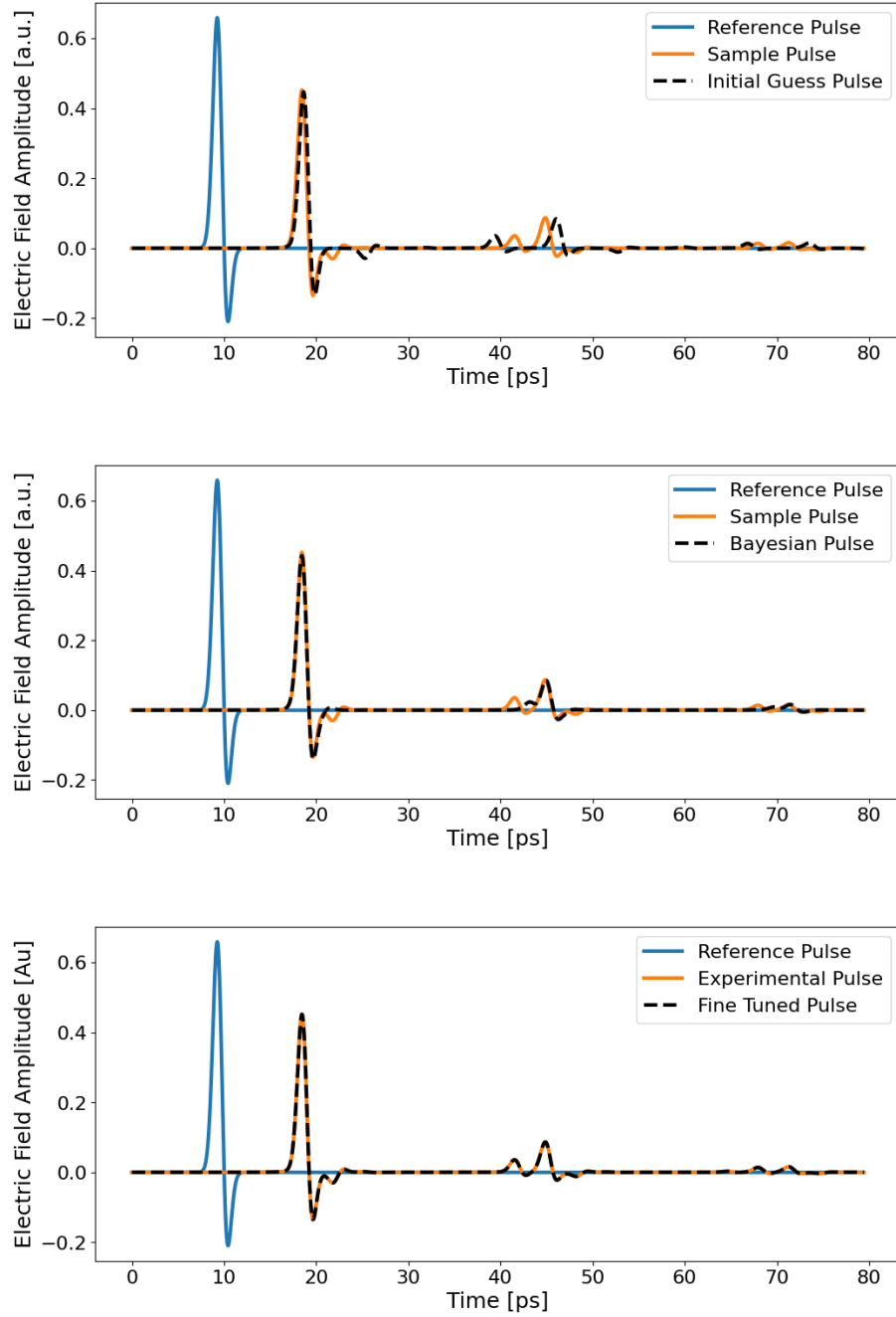


Fig. 4. (a) Time domain of simulated reference and sample pulse for a 2 layered material with material parameters: $n = 3.46 - 0.01i$, $2.5 - 0.015i$ and $d = 1, 0.2$ mm respectively. These were simulated using a transfer matrix methods. The simulated pulse using the initial guess parameters is shown as well (black dashed). (b) For a 2 layered material with material parameters: $n = 3.46 - 0.01i$, $2.5 - 0.015i$ and $d = 1, 0.2$ mm, Bayesian optimisation is shown, the Bayesian optimisation results are $3.34 - 0.014i$, 1.11 mm for layer 1 and $2.7 - 0.016i$, 0.10 mm for layer 2. (c) Using the Bayesian optimization's result as the seed value for the gradient descent converges to $3.4601 - 0.0099i$, 1.0002 mm and $2.5001 - 0.01490i$, 0.20003 mm. The reconstructed pulse using these parameters is shown by the black dashed line.

170 2. Results

171 In order to test the optimisation method, we have performed extractions on a variety of simulated
172 samples. Initial guesses for the material parameters are randomly selected. The algorithms are
173 tested on a 5 layer sample with 15 free parameters (3 per layer). An initial value is randomly
174 selected within a confidence interval of the material parameters. The Bayesian model then
175 searches a space with the following bounds on each material parameters: [n: ± 0.5 , k: ± 0.01 , d:
176 $\pm 50 \mu\text{m}$]. The results from this are then passed to the gradient based model that converges to
177 fine-tune each material parameter.

178 should we include loss vs epoch graphs for with / without Bayesian optimisation?

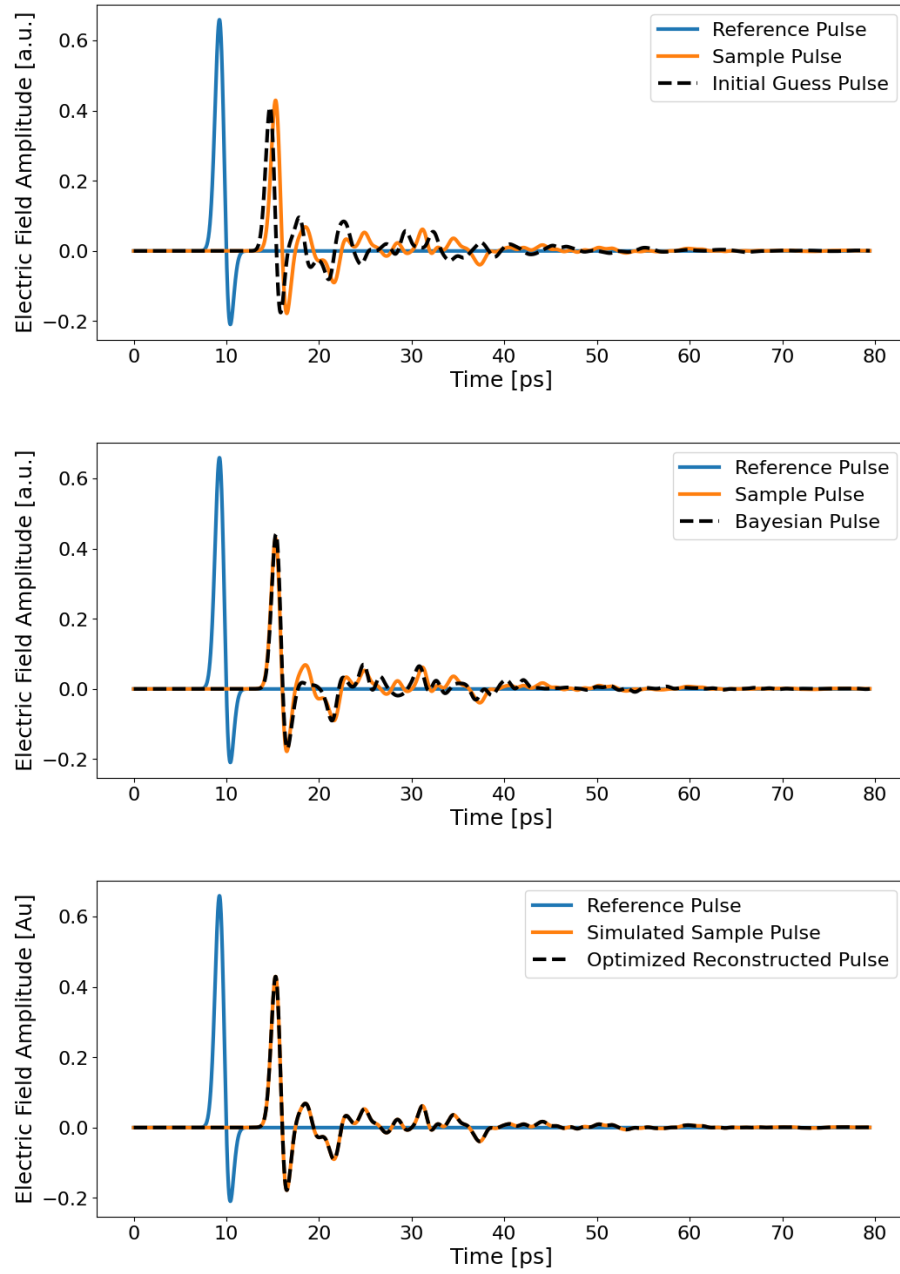


Fig. 5. (a) Time domain of simulated reference and sample pulse for a 5 layered material (b) Bayesian optimisation results with sample pulse and initial guess pulse (c) Using the Bayesian as a first approximation the gradient descent converges to 4th or 5th decimal accuracy

Table 1. Optimization results of a clean pulse from a 5 layer simulated sample.

Layer	n				k				d (μm)			
	n_{true}	n_{fit}	Residual	% Error	k_{true}	k_{fit}	Residual	% Error	d_{true}	d_{fit}	Residual	% Error
1	3.364	3.3653	+0.00127	+0.038%	-0.000356	-0.000399	-0.000043	+12.1%	0.150	0.1500	-0.00005	-0.03%
2	2.522	2.5229	+0.00088	+0.035%	-0.003711	-0.003618	+0.000093	-2.5%	0.179	0.1789	-0.00006	-0.03%
3	5.411	5.4104	-0.00058	-0.011%	-0.005331	-0.005254	+0.000077	-1.4%	0.102	0.1020	+0.00000	0.00%
4	4.213	4.2115	-0.00150	-0.036%	-0.008436	-0.008378	+0.000058	-0.69%	0.206	0.2061	+0.00009	+0.04%
5	1.660	1.6597	-0.00032	-0.019%	-0.009043	-0.008860	+0.000183	-2.0%	0.120	0.1200	+0.00003	+0.02%

183 **References**

- 184 1. P. Yeh, *Optical Waves in Layered Media* (Wiley, 1988).
- 185 2. J.-Y. Zhang, J.-J. Ren, L.-J. Li, *et al.*, “Terahertz spectroscopy and effective medium theory for thickness measurement
186 of adhesive bonds,” *NDT & E Int.* **147**, 103216 (2024).
- 187 3. D. P. Kingma and J. Ba, “Adam: A method for stochastic optimization,” (2017).
- 188 4. C. E. Rasmussen and C. K. Williams, *Gaussian Processes for Machine Learning* (MIT Press, 2006).
- 189 5. J. Mockus, V. Tiesis, and A. Zilinskas, “Application of bayesian approach to numerical methods of global and
190 stochastic optimization,” *J. Optim. Theory Appl.* **34**, 445–459 (1978).
- 191 6. N. Srinivas, A. Krause, S. M. Kakade, and M. W. Seeger, “Gaussian process optimization in the bandit setting: No
192 regret and experimental design,” in *ICML*, (2010).
- 193 7. J. Snoek, H. Larochelle, and R. P. Adams, “Practical bayesian optimization of machine learning algorithms,” (2012).